ISSN 1541-308X, Physics of Wave Phenomena, 2019, Vol. 27, No. 3, pp. 165–177. © Allerton Press, Inc., 2019.

LASER SPECTROSCOPY

Investigation of the Interaction of Water Molecules with the Surface of a Quartz Tube Using Diode Laser Spectroscopy

A. V. Bernatskiy[1*], V. V. Lagunov[1], and V. N. Ochkin[1***]**

[1] *Lebedev Physical Institute, Russian Academy of Sciences, Leninskiy pr. 53, Moscow, 119991 Russia*

Received May 29, 2019; in final form, May 29, 2019; accepted June 5, 2019

Abstract—The behavior of water molecules at the density of 10^{13} to 10^{16} cm^{-3} in a fused silica tube at room temperature has been studied. The number of molecules in the gas phase initially injected in the tube is comparable to the number of molecules adsorbed on the walls of the pre-evacuated tube. The concentrations of molecules in the gas phase were measured by diode laser spectroscopy with an external optical cavity. An off-axis alignment of the cavity with a large set number of transverse modes was used, which made it possible to measure the concentrations of molecules with narrow absorption profiles, temporal resolution of 5 s, and the accuracy better than ±5%. A strong interaction of molecules with the walls was observed. The time behavior of molecules in the gas phase both after the injection of gas into the vacuum volume and after its rapid evacuation under dynamic equilibrium between capture and desorption processes is non-exponential. The characteristic time of these processes 10^{-11} to 10^{2} s depends on the redistribution of molecules between the gas and the near-wall layers, which is governed by the physical and chemical adsorption mechanisms. The theoretical results on the kinetics of the processes are in good agreement with the experimental data.

DOI: 10.3103/S1541308X19030014

1. INTRODUCTION

The capture and release of gas molecules by surfaces of solids has been studied at a quantitative level for more than 100 years [1] as these processes are important for vacuum technology, ecology, medicine, colloid chemistry, gas purification and storage, etc. [2, 3].

Traditionally, the ability to adsorb a substance is studied by sample weighting and drying or similar procedures. Adsorbents with a high specific surface area [cm^2 g^{-1}] are used, which is achieved due to porosity or dispersion of the material. To enhance the effect, reduce the measurement time and improve the accuracy, the adsorbed gas (adsorbate) is maintained at a sufficiently high (usually about 1 atm) partial pressure [4]. On the contrary, in vacuum technology measurements are carried out at low pressure using sensitive pressure sensor; long time (hours, days) is required for the dynamic equilibrium to be established [5, 6]. In some cases, particular techniques are developed, which reveal, for example, changes in the natural frequency of a quartz cavity monitored during adsorption of gas molecules on it [7]. Other methods make use the effect of gas adsorption on electrodes on the current-voltage characteristics and on self-oscillations [8] in plasma studies.

In recent years, the interest in the experimental study of adsorption has grown, in particular, when employing plasma-vacuum devices for controlled chemical reactions as well as in nuclear fusion energy facilities. In plasma-vacuum technologies, the knowledge of behavior of water molecules is essential due to their high adhesion and abundance. For example, the project of the ITER design [9] suggests that the change in the content of water molecules (their flux) in the operation chamber should not exceed 10^{-7} Pa m^3 s^{-1}, which undoubtedly requires taking into account the role of adsorption and desorption. This, in particular, was shown in [10] in the experiments simulating the behavior of molecules near cooled walls of the reactor. For many devices, the gas or plasma medium and the surrounding surfaces are difficult to evaluate for contact analysis, which contributed to the problem of the development of special methods for remote spectroscopy [11–18].

In parallel with the development of experimental methods, a theory of adsorption was elaborated with its own system of basic concepts and laws. One should distinguish physical and chemical adsorption

*E-mail: bermen@mail.ru
**E-mail: lagunoww@yandex.ru
***E-mail: ochkin@sci.lebedev.ru

mechanisms [1, 2]. Both mechanisms are due to an excess of surface free energy. From the viewpoint of thermodynamics, these mechanisms differ only by the interaction energy (heat of adsorption), although additional factors are taken into account in a more detailed description. Physical adsorption mechanism is associated with the presence of relatively long-range van der Waals (vdW) forces, among which the main ones are dispersion, induction, and orientational forces [3]. In the case of physical adsorption, the properties of a molecule near the surface are not changed. During chemical adsorption, an initially independent molecule shares its electron with a particle of the adsorbing layer. In that case, the potential well depth is typically 0.5 to 5 eV; and at room temperature, the molecules stay at the surface for a long time. During physical adsorption, typical well depths are 0.04 to 0.4 eV, the desorption time is short, the process is easily reversible and, if the gas consists of particles of different types, they can replace each other in the surface layer.

The most widely used "basic" adsorption models establish the relationship between the number of particles captured by the surface and the number of particles in the gas phase at stationary conditions. Corresponding expressions are adsorption isochors or isobars, but more often, adsorption isotherms are used. The Langmuir isotherm

$$V_{\mathrm{p}} = \frac{V_{\mathrm{m}} b p}{1 + bp} \qquad (1)$$

is a special one in the sense that it applies to both physical and chemical adsorption under certain assumptions. Here V_{p} is the volume of the adsorbed substance at a partial gas pressure p, V_{m} is the volume of the maximum number of molecules that can be captured by the surface (usually taken as one monolayer), and b is an empirical constant depending on the temperature.

The Brunauer–Emmett–Taylor (BET) isotherm for multilayer adsorption [19] and the Freundlich empirical isotherm [2] are best known among other relations that extend the conditions of applicability for formula (1). It is usually assumed that the number of adsorbed particles is smaller than the number of particles in the gas phase. In this case, the gas pressure during establishing the equilibrium is almost constant. According to Freundlich, the volume V_{p} of the adsorbed substance is related to the gas pressure p as

$$V_{\mathrm{p}} = sp^{l}, \qquad (2)$$

where s, l are the model parameters. The values of l are in the range of 0.1 to 0.9 and grow with the temperature, s depends on the type of the gas–adsorbent pair.

In contrast with the Langmuir isotherm, the BET isotherm includes a constant C that depends on the difference between the adsorption and condensation potentials U_{a} and E, respectively:

$$V_{\mathrm{p}} = \frac{p}{p_0 - p} V_{\mathrm{m}} C \left[1 + \left(1 - \frac{1}{C}\right)\frac{p}{p_0}\right]^{-1}, \qquad (3)$$

here $C = \exp[(U_{\mathrm{a}} - E)/kT]$ and k is the Boltzmann constant.

These and other isotherms are often used to obtain the amount of the adsorbed gas or, if known, to determine the absorbent actual specific surface, which may differ significantly from the geometric one due to surface roughness, porosity, etc. [3]. For example, in [20, 21], it was found that for the steel of the vacuum chamber this difference is 5.8 on the average.

A common feature for the considered and similar thermodynamic models is that they provide a means to determine only stationary relationships between particle concentrations on the surface and in the gas phase. Moreover, the prevailing adsorption mechanism is assumed to be known, and all models rely on this fact. In this case, the origin of the isotherm is almost not considered, and the experimental approaches described above can hardly be used to derive the isotherms.

In this work, we first consider the time behavior of the concentration of water vapor in a fused silica tube using diode laser spectroscopy (DLS) which has been extensively studied in recent decades [14]. Such tubes are often used for gas transport and storage, as well as for generating plasma, conducting chemical reactions, designing chemical and gas-discharge lasers, etc. The results are analyzed in terms of the developed model for kinetic interaction of molecules with the surface during the physical and chemical adsorption. In this case, the number of particles in the gas phase during establishing dynamic equilibrium varies and is comparable to the number of trapped molecules which also varies.

2. EXPERIMENT AND MEASUREMENT TECHNIQUE

The schematic representation of the experimental installation is shown in Fig. 1. It is a modification of the installation described in [22]. Adsorption was studied in a water-cooled quartz tube *1* with a length of 45 cm and an internal diameter of 2 cm. The residual pressure was 5×10^{-5} Torr and was achieved using a TDS-022 Pfeiffer pumping station *2*. From a 150 ml glass flask *3* partially filled with water, water vapor was let into the container *5* (30 ml). Container *5* was isolated by a vacuum valve and the water vapor pressure in the container was monitored by a pressure sensor *5a* (Pfeiffer TPR250). Since the ratio of the

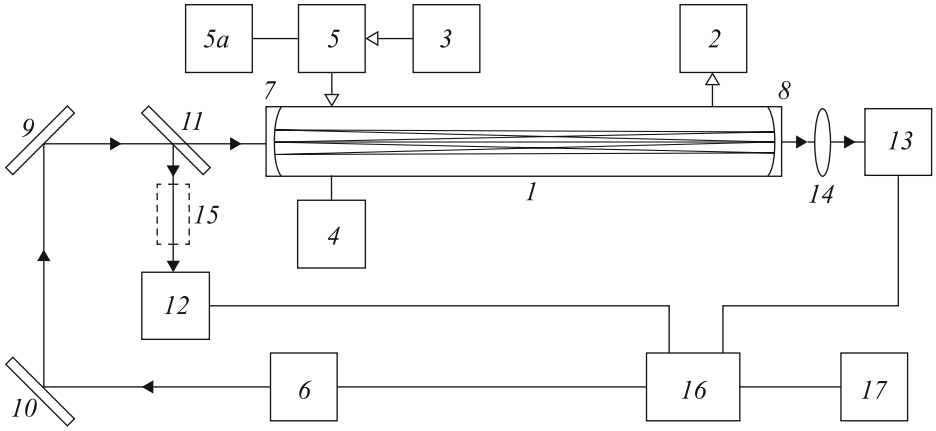

Fig. 1. Installation scheme. Designations are given in the text.

volumes of the tube and the container *5* was known, the desired number of water molecules was injected into the tube. The process was additionally monitored by a Thyracont VSM77DL pressure sensor *4*. The water vapor content in the tube, as well as its dynamics, were accurately measured by laser spectroscopy.

The need for laser measurements is dictated by the fact that, according to the specifications of the sensors provided by the manufacturers, the accuracy of pressure measurements with modern sensors (including those used in this work) in the concentration range of our interest, 10^{16} to 10^{13} cm^{-3}, is limited and ranges from 15 to 50%.

Figure 1 also shows the optical measurement unit. To extend the optical path, we place mirrors *7* and *8* with curvatures of 1 m at the ends of the tube, thus forming an optical cavity. According to the manufacturer data (Layertec), the reflectivities of the mirrors were higher than 99.98% in the wavelength range from 1300 to 1400 nm. This corresponds to the effective optical path length $L = 3100$ m. The radiation of laser *6* was injected into the cavity at a small angle by mirrors *9* and *10*. One of the reasons for using the off-axis alignment is that, at low pressures, the widths of the Doppler profiles of the absorption lines are comparable to the spacing between the axial cavity modes. Therefore, it is difficult to determine the position of the mode on the profile of the absorption line. This made the accuracy of the absorption measurement unacceptable. The advantage of the employed scheme is that a large number of transverse modes fall within the transmission spectrum [23, 24]. Thus, the transmission spectrum can be considered as continuous in the frequency tuning band, and it is possible to measure the absorption by both discrete (at a specified point of the profile) and integral methods. According to our estimates, the density of the resonator modes is about 10^3 cm^{-1}.

An Eblana Photonics DM-1392 tunable diode laser *6* emitting at 1392 nm with power of up to 8 mW and the linewidth of 2 MHz (about of 10^{-4} cm^{-1}) was used. A Peltier element maintained the temperature of the laser at 303 K. The laser operated in a repetitively pulsed regime from 50 to 200 Hz. The frequency was tuned by injecting pump current pulses of a specific shape shown in Fig. 2(a) (for a repetition rate of about 200 Hz). Zero-current interval of 0.5 ms sets the time between the successive pulses. The zero-current interval is followed by a current plateau (30 mA) with the duration of 1.5 ms to achieve the threshold current and establish the initial tuning frequency. The subsequent linear increase in the current from 30 to 115 mA over about 3 ms provides frequency tuning. Then, the current drops rapidly ($\approx 1\,\mu$s). Within the pulse, the current changes discretely with a step of 1 to 1.5 μs. The entire tuning range is 2 cm^{-1}, the amplitude of the pulses is 115 mA, the period is 5 ms. Figure 2(b) shows a typical absorption spectrum of water. A scaled up absorption line is shown in Fig. 2(c), Gaussian approximation of the line is also presented. Since at experimental pressures the line profiles can be considered as Doppler ones with good accuracy, the gas temperature can be obtained from the width of the Gaussian curve. This temperature was determined for each recorded spectrum that was possible due to the off-axis alignment. Since the temperature of the cooling tube varied, the gas temperature fluctuated within 295 to 302 K over the long-run measurements. The signals from the cavity output detector *13* were converted to digital format with a PCI-6120 multifunctional I/O board (National Instruments) *16* and processed by a computer *17*.

Particle concentrations were determined using the Bouguer–Beer–Lambert law $I = I_0 \exp(-\alpha L)$ (α is the absorption coefficient and L is the optical path length) for integral absorption [25, 26]:

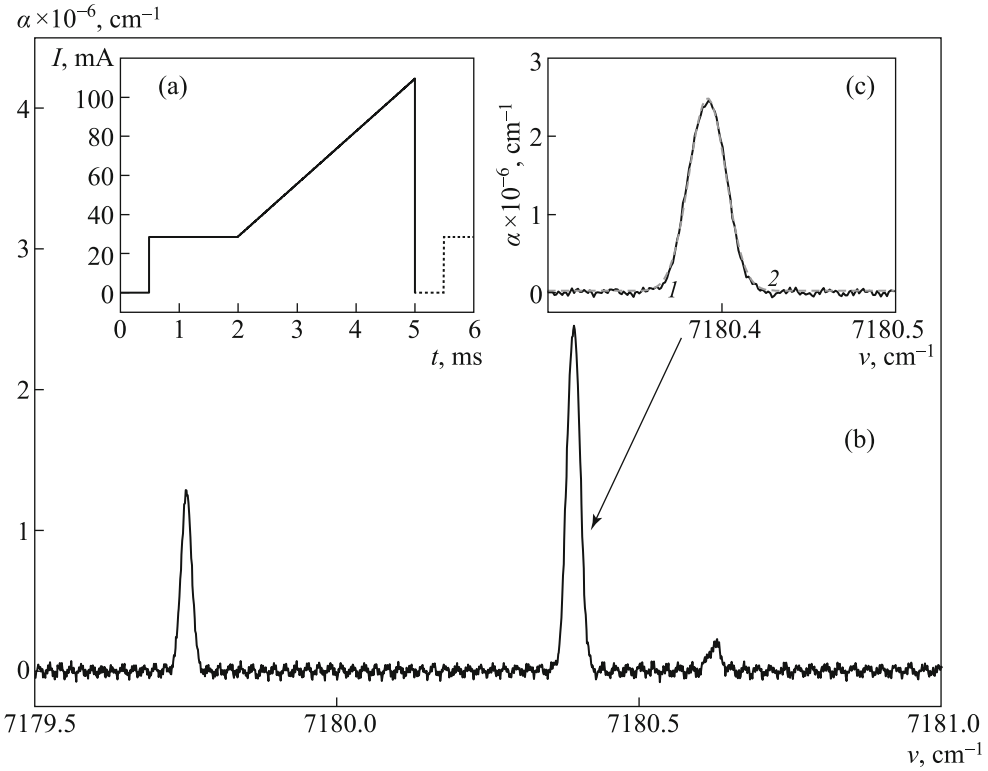

Fig. 2. (a) Pulse shape of the injection current; (b) a fragment of the absorption spectrum; and (c) absorption line profile: experiment (*1*) and Gaussian approximation (*2*).

Table 1. Characteristics of the used H_2O absorption lines

Wavenumber, cm^{-1}	Line intensity, 10^{-23} cm mol^{-1}	Transition	Q_{rot} (295 K)	Q_{rot} (302 K)
7179.75	17	$Q(7)(000-101)$	173.7	179.9
7180.39	55.6	$P(4)(000-002)$	173.7	179.9
7801.61	2.95	$Q(9)(000-101)$	173.7	179.9

$$n = \frac{Q_{rot}}{S_{lu}} \int_{\nu} \ln\left[\frac{I_0(\nu)}{I(\nu)}\right] d\nu. \qquad (4)$$

Here u and l stand for, respectively, the rotational numbers for the upper and lower levels of the vibrational–rotational transition; I_0 and I are, respectively, the intensities of the laser radiation at the cavity input and output; S_{lu} is the intensity of the line [cm mol^{-1}] for the corresponding transition; and Q_{rot} is the rotational partition sum (at room temperature there is no need to take into account the vibrational and electronic components of the total partition function).

To achieve an acceptable concentration range, several vibrational–rotational transitions were considered. They are listed in Table 1 along with the intensities of the corresponding lines [25, 26] and the partition sums [27] for the temperature limits in our experiment.

For concentration measurements under different conditions, we selected the lines for which the ratio I_0/I was within 0.2 to 0.5. At these values, the errors are minimal [28, 29].

3. EXPERIMENTAL RESULTS

We have carried out 15 independent runs of measurements to obtain the temporal dependencies $n(t)$ of the concentrations of H_2O molecules for different initial gas concentrations $n_0 = n(t=0)$ in the preevacuated tube at different observation times and pumping modes. Figure 3 shows the examples on a semilogarithmic scale. These examples correspond to the observation intervals of 360 and 600 s and initial concentrations $n_0 = 3-7.2$ cm^{-3}. The symbols stand for the experimental data; the accuracy is ±5%. Solid curves are B-spline approximations of the experimental data.

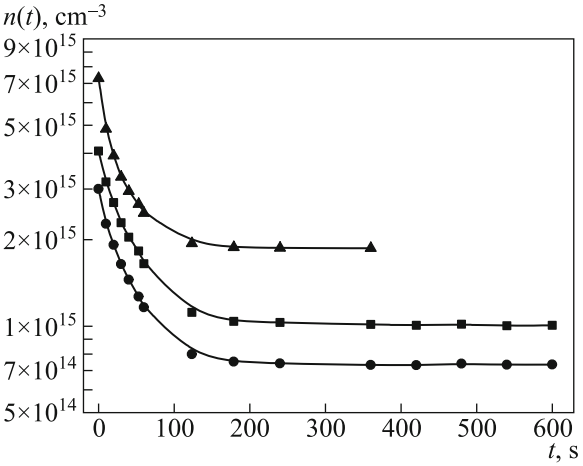

Fig. 3. Decrease in the concentrations of H_2O molecules for different values of n_0: 3×10^{15} (■), 4×10^{15} (●), and 7.2×10^{15} cm^{-3} (▲).

Qualitative analysis shows that the dependencies are non-exponential but have similar behavior. First, a drop is observed over 0 to 200 s, and then the dependencies become stationary ($n_{\rm st}$). The obtained dependences can be described by the general formula

$$n(t) = n_{0i}\exp\left(-\frac{t}{\tau_i}\right) + f_i(t) + n_{{\rm st},i}. \qquad (5)$$

Graphical differentiation of (5) shows that the first term corresponds to an exponential decrease over the interval of 0 to 10 s; here $\tau_1 \approx \tau_2 \approx \tau_3$. For this example, it also turns out that within the measurement errors $n_{\rm st1}: n_{\rm st2}: n_{\rm st3} \approx n_{01}: n_{02}: n_{03}$. In contrast, the functions $f_i(t)$, which determine the transition period, differ from each other, although they can also be approximated by exponentials.

The reported results are purely empirical. To understand what processes are responsible for their description in the formula (5), how the above relations between times and concentrations are justified and what interactions determine the characteristic times τ_i and the behavior of $f_i(t)$, as well as to explain some additional experimental facts, a more detailed consideration of the kinetics is required.

4. KINETICS OF PARTICLES AFTER VAPOR ADMISSION INTO AN EMPTY TUBE

Let $n_0 = n(t=0)$ be the initial concentration of water molecules in the gas phase in the tube, with $n_{\rm p}$ and $n_{\rm c}$ corresponding to the number of molecules physically and chemically adsorbed on a unit area of an ideally smooth quartz surface [cm^{-2}]. The values $\tau_{\rm pa}$, $\tau_{\rm pd}$ and $\tau_{\rm ca}$, $\tau_{\rm cd}$ are the characteristic times of physical (p), chemical (c) adsorption (a) and desorption (d), respectively. Let us assume that the kind of the adsorbed molecule does not change at its subsequent desorption. When the particles are transferred from the surface into the volume, the ratio between the surface [cm^{-2}] and bulk [cm^{-3}] densities is S/V; for a cylindrical tube, we have $S/V = 2/R$ [cm^{-1}]. In addition, the real surface is rough and porous [2], and the actual average surface density of the particles is $\widetilde{n} = Fn_{\rm s}$; therefore, the condition for particle balance in a closed volume is

$$n_0 = n(t) + \frac{2F}{R}\left[n_{\rm p}(t) + n_{\rm c}(t)\right]. \qquad (6)$$

Given a geometric factor $2F/R = \gamma$ [cm^{-1}], the balance equation for the processes has the form

$$\frac{dn}{dt} = -\frac{n}{\tau_{\rm pa}} - \frac{n}{\tau_{\rm ca}} + \gamma\left(\frac{n_{\rm p}}{\tau_{\rm pd}} + \frac{n_{\rm c}}{\tau_{\rm cd}}\right). \qquad (7)$$

Eliminating $n_{\rm c}$ using the condition of particle balance (6), we rewrite equation (7) in the form

$$\frac{dn}{dt} + \frac{n}{\tau^*} = \gamma\frac{n_{\rm p}}{\tau^{**}} + \frac{n_0}{\tau_{\rm cd}}, \qquad (8)$$

where

$$\frac{1}{\tau^*} = \frac{1}{\tau_{\rm pa}} + \frac{1}{\tau_{\rm ca}} + \frac{1}{\tau_{\rm cd}}, \qquad (9)$$

$$\frac{1}{\tau^{**}} = \frac{1}{\tau_{\rm pd}} - \frac{1}{\tau_{\rm cd}}. \qquad (10)$$

To integrate Eq. (8), we need to obtain the $n_{\rm p}(t)$ dependence. When a particle is transferred from the volume to the surface, it can be trapped in the layer formed by physical adsorption with probability α and remain there for $\tau_{\rm pd}$ which is a characteristic time of the desorption process at the particle release from the vdW potential well.

Provided that $N_{\rm m}$ molecules are placed on a unit surface area with a dense filling of the monolayer and each location (center) can capture a particle by the physical mechanism, while the other centers are free, the particle will be trapped at the surface with probability α_0. If the fraction of occupied centers is $\theta = n_{\rm p}/N_{\rm m}$, then the trapping probability is $\alpha = \alpha_0(1-\theta)$. According to the kinetic theory of gases, the frequency of single passes of molecules through a unit area in the volume (or the frequency of molecular collisions with a unit surface area) is

$$\nu = n\sqrt{\frac{kT}{2\pi M}}, \qquad (11)$$

k is the Boltzmann constant, T is the gas temperature, and M is the molecule mass. Then, the density of particles $n_{\rm p}$ in the layer formed by physical adsorption is found from the equation

$$\frac{dn_{\rm p}}{dt} = \alpha\nu - \frac{n_{\rm p}}{\tau_{\rm pd}}. \quad (12)$$

This is a first-order non-homogeneous differential equation of the type

$$\frac{dy}{dx} = py + g(x) \quad (13)$$

that has a general solution [30, 31]

$$y = C\exp(px) + \int_{x_0}^{x} \exp\bigl[p(x-\xi)\bigr] g(\xi)\, d\xi, \quad (14)$$

where C is a constant. When $x = \mathrm{t}$, $x_0 = 0$ and at the initial condition $n_{\rm p}(t=0) = 0$, the solution of Eq. (12) is

$$n_{\rm p}(t) = \alpha\nu\tau_{\rm pd}\left[1 - \exp\left(-\frac{t}{\tau_{\rm pd}}\right)\right] \quad (15)$$

or

$$n_{\rm p}(t) = n_{\rm p}^0\left[1 - \exp\left(-\frac{t}{\tau_{\rm pd}}\right)\right]. \quad (16)$$

The maximum possible number of molecules adsorbed on a unit surface area at $t \to \infty$ is

$$n_{\rm p}^0 = \alpha_0(1-\vartheta)\,\tau_{\rm pd} n\sqrt{\frac{kT}{2\pi M}} \quad (17)$$

and, generally speaking, it is not equal to the maximum possible density of particles $N_{\rm m}$ that can potentially be adsorbed on the surface (for example, at a particular time the number of absorbing centers is not equal to the number of molecules in a densely packed monolayer because some of these centers are already "involved" into the chemical adsorption). Relation (17) can be rewritten in the form that coincides with the formula of the Langmuir isotherm (1) with b replaced by g and the volume of adsorbed particles V replaced by their number n with $p = nkT$:

$$\frac{n_{\rm p}^0(T)}{N_{\rm m}} = \frac{g(T)\,n}{1 + g(T)\,n}, \quad (18)$$

$$g(T) = \alpha_0\frac{\tau_{\rm pd}}{N_{\rm m}}\sqrt{\frac{kT}{2\pi M}}. \quad (19)$$

Equation (18) differs from (1) by that the instantaneous surface density $n_{\rm p}^0$ depends explicitly on the temperature and can be used to solve the kinetic equation (8):

$$\frac{dn}{dt} + n\left(\frac{1}{\tau^*} - \gamma\frac{N_{\rm m}}{\tau^{**}}\frac{g}{1+gn}\right) = \frac{n_0}{\tau_{\rm cd}}. \quad (20)$$

In contrast to Eq. (12), Eq. (20) is nonlinear relative to the desired variable $n(t)$. Its solution cannot be expressed in elementary functions, and numerical methods are required to solve it. However, under certain conditions, Eq. (20) allows physically justified linearization. For this purpose, let us estimate the value g by formula (19) for a water molecule. Here we assume that the probability for physical adsorption on a "clean" surface not occupied by other adsorbed molecules is $\alpha_{0\rm p} = 1$ (maximum possible). The time of physical desorption is traditionally [1–3] estimated according to the well-known relation $\tau_{\rm pd} = \tau_0\exp(U_{\rm d}/kT)$ proposed by Frenkel with $U_{\rm d}$ being the depth of the vdW potential and τ_0 being the time required for the molecule to move along the surface from one adsorption center to another. The typical value of τ_0 corresponds to the time of oscillation of atoms in the potential well of a molecule, i.e., $\tau_0 \approx 10^{-13}$–10^{-12} s. According to the data of [7], the vdW potential for water on quartz is about $U_{\rm d} = 0.14$ eV and, at a temperature of 300 K, the corresponding time $\tau_{\rm pd}$ is about 10^{-10} s, while the value of g is $\approx 10^{-20}$ cm^3. Under our experimental conditions, the concentration of molecules in the gas phase is $n \approx 10^{13}$–10^{16} cm^{-3} and $gn \ll 1$; therefore, Eq. (18) can be reduced to a linear equation of the type (12) that is more convenient for analysis.

If we introduce the designation

$$\frac{1}{\tau^{***}} = \frac{1}{\tau^*} - \gamma N_{\rm m}\, g\frac{1}{\tau^{**}} = \frac{1}{\tau_{\rm pa}} + \frac{1}{\tau_{\rm ca}} + \frac{1}{\tau_{\rm cd}} - \gamma N_{\rm m}\, g\left(\frac{1}{\tau_{\rm pd}} - \frac{1}{\tau_{\rm cd}}\right), \quad (21)$$

then, in accordance with (14), after integration from 0 to t, the solution of the linearized equation (20) with the initial condition $n(t=0) = n_0$ will be

$$n(t) = n_0\left\{\exp\left(-\frac{t}{\tau^{***}}\right) + \frac{\tau^{***}}{\tau_{\rm cd}}\left[1 - \exp\left(-\frac{t}{\tau^{***}}\right)\right]\right\}. \quad (22)$$

At longer times ($t \to \infty$), the concentration of the molecules reaches the stationary level

$$n^{\rm st} = n(\infty) = n_0\frac{\tau^{***}}{\tau_{\rm cd}}. \quad (23)$$

Relations (21)–(23) explain the behavior of the dependencies in Fig. 3, the empirical formula (5), the relations between its parameters and their meaning, as well as the form of the "transition" function f_i in (5). The characteristic time $\tau^{***} \approx \tau_1 \approx \tau_2 \approx \tau_3$ (see Sec. 3) can be found by differentiating the experimental dependences $n(t)$ for small t, then the time of chemical desorption is determined by formula (23). Below we discuss other parameters involved in the expressions in Sec. 4.

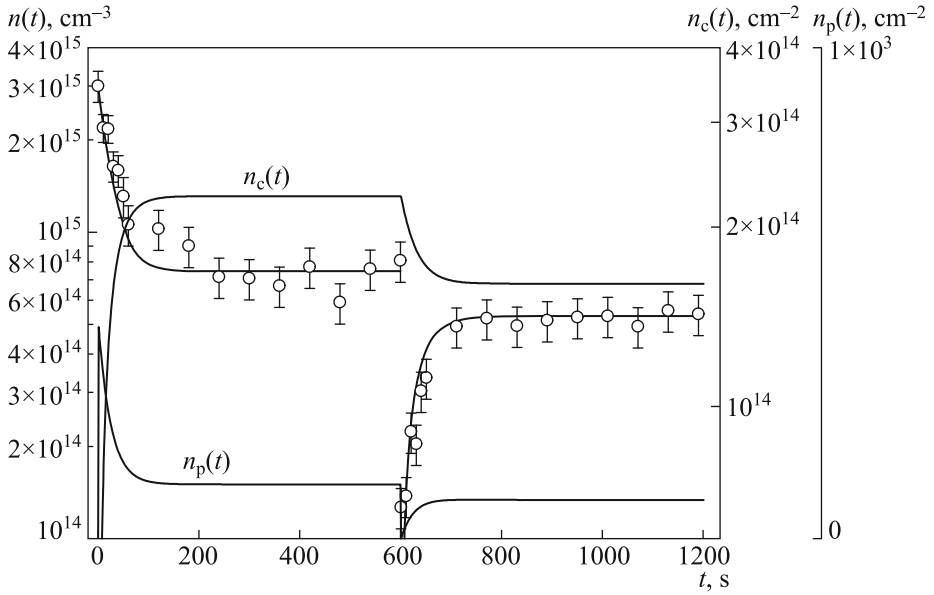

Fig. 4. Dynamics of the particle concentration n in the gas phase and their surface density in the layers formed by physical and chemical adsorption (n_p and n_c, respectively). Circles stand for the measurement results (DLS method) and solid curves represent calculation results.

5. BEHAVIOR OF PARTICLES IN THE GAS PHASE AFTER SHORT-TIME PUMPING

As can be seen from the dependencies in Fig. 3, by the time T, in 3–5 min after particle injection into an empty tube, the concentration of water molecules in the gas phase reaches a stationary level $n^\mathrm{st} = n^T$. By this time, some of the molecules are in the surface layers formed by "physical" and "chemical" adsorption, and the concentrations of these molecules also reach the stationary values n_p^T and n_c^T, i.e., dynamic equilibrium is established. This means that the rates of particle capture and release by the wall layers are leveled off. We have carried out the experiments in which, after the dynamic equilibrium was established at time T, the molecules were quickly (1 to 3 s) pumped out in a period shorter than the time of the concentration measurements for the molecules in the gas phase. The tube was evacuated to $\approx 10^{-3}$ Torr (to a water concentration of about $3\times10^{13}\,\mathrm{cm}^{-3}$). Results of this experiment are shown in Fig. 4.

It is possible that during the pumping, the molecules from the layer formed by physical adsorption are also removed, since the time of physical desorption τ_pd is short, as mentioned above. Here we should note the following. First, the concentration of particles in the "physical" layer is small, which follows from formula (18) at $gn \ll 1$. Second, due to the short adsorption–desorption times, this layer will be rapidly restored immediately after the pump is switched off and the adsorbed molecules are released. Therefore, we assume that after short-time pumping, the number of molecules in the surface layers remains equal to that before the pumping started. For brevity, we also take $T = 0$ as the starting point. After pumping has stopped, molecules in the gas phase begin to appear in the volume as a result of desorption. The corresponding variables n at $t > T$ are primed.

Changes in the particle concentrations after pumping are formally described by an equation which is similar to (5). However, under alternative initial conditions, a different balance of particles, and new combinations of the process rates with generalized characteristic times τ_pa, τ_pd and τ_ca, τ_cd, we have

$$\gamma n_\mathrm{c}^T + \gamma n_\mathrm{p}^T = \gamma n'_\mathrm{p}(t) + \gamma n'_\mathrm{c}(t) + n'(t). \qquad (24)$$

Taking into account (24) and relations (17)–(21), it is more convenient to rewrite the kinetic equation (7) in the form

$$\frac{dn'}{dt} = -n'\left(\frac{1}{\tau_\mathrm{pa}} + \frac{1}{\tau_\mathrm{ca}} - \gamma\alpha\sqrt{\frac{kT}{2\pi M}}\right) + \gamma\frac{n'_\mathrm{c}}{\tau_\mathrm{cd}}. \qquad (25)$$

The expression for concentration n'_c is found from the equation

$$\frac{dn'_\mathrm{c}(x)}{dx} = -n'_\mathrm{c}(x)\frac{1}{\tau_\mathrm{cd}} + \frac{n'}{\gamma}\frac{1}{\tau_\mathrm{ca}} \qquad (26)$$

similar to how it was done above for n_p (12), (16), and (17).

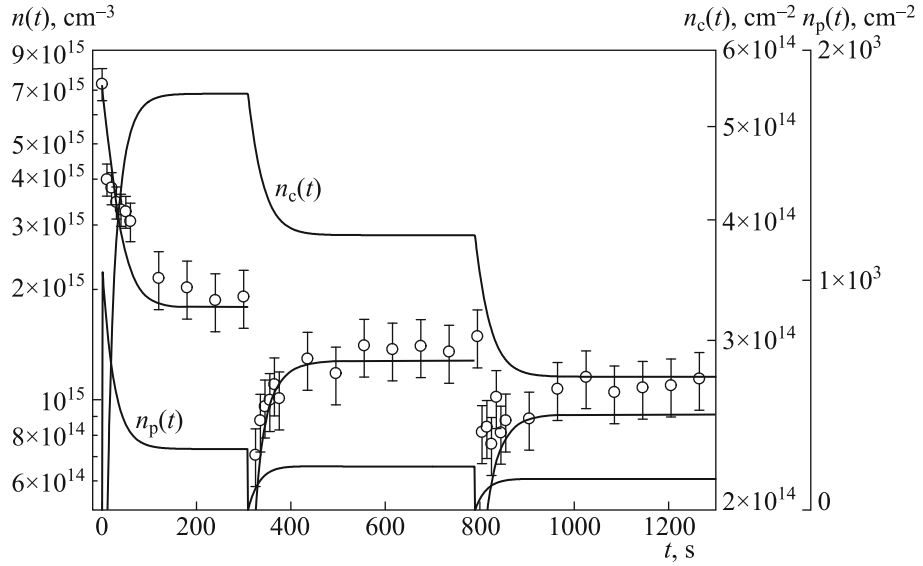

Fig. 5. Dynamics of concentrations and surface densities of molecules in the experiment with double intermediate pumping at T and T_1. Notations are similar to Fig. 4.

Under the initial condition $n_c(T=0)=n_c^T$, with $1/\tau'''=1/\tau_{cd}+1/\tau_{ca}$, and with $n_p^T, n_p \ll n_c^T, n_c$, $gn \ll 1$ taken into account, the solution of Eq. (26) is

$$n_c'(x)=n_c^T\left\{\exp\left(-\frac{x}{\tau'''}\right)+\frac{\tau'''}{\tau_{ca}}\left[1-\exp\left(-\frac{x}{\tau'''}\right)\right]\right\}. \tag{27}$$

In this case, the general solution of Eq. (25) has the form

$$n'(t)=C\exp\left(-\frac{t}{\tau'}\right)+n_c^T\frac{\gamma}{\tau_{cd}}\left\{\tau''\left[\exp\left(-\frac{t}{\tau'}\right)-\exp\left(-\frac{t}{\tau'''}\right)\right]\right.$$
$$\left.\times+\frac{\tau'''\tau'}{\tau_{ca}}\left[1-\exp\left(-\frac{t}{\tau'}\right)\right]-\frac{\tau''\tau'''}{\tau_{ca}}\left[\exp\left(-\frac{t}{\tau'}\right)-\exp\left(-\frac{t}{\tau'''}\right)\right]\right\}. \tag{28}$$

Here

$$\frac{1}{\tau''}=\frac{1}{\tau_{pa}}-\frac{1}{\tau_{cd}}-\gamma\alpha\sqrt{\frac{kT}{2\pi M}}, \tag{29}$$

$$\frac{1}{\tau'}=\frac{1}{\tau_{pa}}+\frac{1}{\tau_{ca}}-\gamma\alpha\sqrt{\frac{kT}{2\pi M}}, \tag{30}$$

with the initial condition $n'(t=T=0)=C=0$.

When a new stationary value of n' is achieved after pumping, we have

$$n'(t\to\infty)=n_c^T\frac{\gamma}{\tau_{cd}}\frac{\tau'''\tau'}{\tau_{ca}}. \tag{31}$$

Thus, we conclude that the proposed scheme gives a satisfactory description of the dependencies in Fig. 4. In the interval $(0,T)$, formulas (6), (16), (17), (19), (22), and (23) are applicable, and while at $(T,+\infty)$, formulas (24), (27), (28), and (31) are true.

Experiments were also carried out with repeated short-time pumping (Fig. 5) at longer times $T_1>T$. At times longer than T_1, the behavior observed for the molecules in the gas and the layers is quite similar to that described above for the interval $(T,+\infty)$. The corresponding calculations based on relations (24)–(31) are in good agreement with the experiment and are relevant upon replacing n', n_p', n_c', n_c^T with n'', n_p'', n_c'', $n_c^{T_1}$. In this case, it is necessary to fit the parameters involved in the above relations.

6. PROCESS RATES, APPROXIMATION PARAMETERS

Dependencies shown in Figs. 4 and 5 were calculated using the expressions from Secs. 4 and 5. These expressions contain a large number of physical parameters and their combinations. Some of them can be determined directly from the experimental results

and interpreted within the framework of the kinetic model given above. According to the available data, information about other parameters is usually rather fragmentary and refers to different adsorbent–adsorbate pairs with the samples prepared by different techniques. These parameters often have noticeable discrepancies and thus can be considered only as estimates. However, they can be varied within the scatter intervals of the available information and refined based on the condition of optimal approximation of the experimental results.

We can divide the parameters used above into independent ones, those involving combinations of the parameters, and fitting parameters. The latter are not known a priori from the experimental conditions. Together, the considered parameters determine the desired values characterizing the adsorption dynamics.

The independent parameters include characteristic times τ_{p0}, τ_{pa}, τ_{pd}, τ_{ca}, τ_{cd}, the number of molecules N_m in a single layer per unit area, the frequency ν of single passes of molecules through a unit area for a given density, mass and temperature of the molecules.

The combinations of independent characteristic times describing the reduction in the concentration of molecules in the volume due to their transfer to the surface are τ^*, τ^{**}, τ^{***}. The release of molecules from the surface into the volume is characterized by combinations τ', τ'', τ'''. We did not study the detailed surface structure (including micropores), the surface roughness, and the spatial inhomogeneity of these quantities independently and describe them by the aggregate geometric fitting parameter γ. This parameter includes the ratio of the surface and volume density of molecules $2/R$ as well as the ratio of the area of a real rough surface to the geometric area.

The probability for a molecule to be captured by the surface is $\alpha = \alpha_0(1-\theta)$ (see text above formula (9)). For physical adsorption on a clean surface, it is often considered that $\alpha_0 = 1$ since the capture of molecules by the surface on which all adsorption centers are free is an activationless ($E_a = 0$) process [32]. However, as noted above, a significant part of the surface can be occupied by the molecules held by chemical bonds, and it is natural to assume that $\alpha_0 < 1$. The fraction of occupied centers θ also depends on multiple experimental factors including the quality and time of the evacuation, the conditions of previous experiments, the method of surface treatment, etc. Therefore, the factor α should be generally taken as a fitting parameter, as well as the factor g (17), which depends on α. To calculate the probability of "chemical" adsorption, it is necessary besides the factor $(1-\theta)$ to take into account the activation energy of adsorption at individual centers E_{ac}:

$$\alpha_0^C = \alpha_0 \exp\left(\frac{E_{ac}}{kT}\right), \tag{32}$$

for water on quartz $E_{ac} = 280\ \mathrm{erg\,cm^{-2}} = 0.37$ eV [33].

Experimental parameters were averaged over 15 measurements with the initial concentrations of water molecules in the tube being $(3-8)\times 10^{15}\ \mathrm{cm^{-3}}$. The relevant information for temperature $T = 300$ K is given in Table 2.

When choosing the parameters, one can determine, for example, τ^{***}. This can be done in several ways using the experimental data. First, for times $t < \tau^{***}$, τ^{***-1} is directly obtained from the slope of dn/dt (initial slope). The time interval 0–10 s is taken, which is close to the measurement time. At times corresponding to the establishment of stationary concentrations of molecules $n_{st} = n_c^T \approx n(\infty)$, τ_{cd} is determined by formula (23) using values of n_{st} and n_0, with τ^{***} obtained from the initial slope.

Let us discuss the method for estimating the values of the factor g, with this factor depending, among other things, on the probability of a molecule capture on the surface. For physical adsorption on a clean surface, α_0, is considered to be equal to unity in various estimates since the molecule capture by the surface on which all adsorption centers are free is an activationless process [32]. As noted above, most of the surface can be occupied by molecules held by chemical bonds, and it is natural to assume that $\alpha_0 < 1$. This value should also be considered as the fitting parameter. When calculating τ^{***} by formula (22), the value of τ_{cd} was used and the fitting parameter $\alpha = \alpha_0(1-\theta) = 10^{-7}$ was introduced for the correction of τ_{pa} to obtain the value of τ^{***} consistent with the results of the previous measurements. In addition to the time of "delivery" of molecules to the surface, see (12) and (14), parameter α also takes into account the fact that a significant part of the surface is occupied by molecules with relatively low mobility, which are held by chemical bonds. All N_m centers are still able to capture particles via physical adsorption but, for most of the particles, the time to occupy these centers is short, so the probability α_0 of the vdW capture at collisions of the molecules with the surface is also small. Chemical adsorption time τ_{ca} is chosen in a similar way. However, to calculate the probability of "chemical" adsorption, alongside with the spatial factor $(1-\theta)$, the adsorption activation energy E_a should be taken into account:

$$\alpha_0^C = \alpha_0^P \exp\left(\frac{E_a}{kT}\right).$$

Here $\alpha_0^P = 1$ corresponds to the probability of the vdW capture on a clean surface [22], $E_a = 285\ \mathrm{erg\,cm^{-2}} = 0.374$ eV [23]. These values (see Table 2) are used for the calculations by formulas (24)–(26).

Table 2. Values of the parameters used in the calculations and combinations of the parameters

Parameter	Variation range	Determination method	Comment	Selected value
γ	2–10	$2F/R=\gamma$ (4), (5)	F is the fitting parameter of the surface roughness. $F=5$ for a tube with an inner radius $R=1$ cm, which is close to the data for steel $F=5.8$ [7, 8]. γ matches parameter τ^{***} determined independently (21)	10±0.07
N_{m}	4×10^{14} cm^{-2}	The ratio of unit surface area to the effective area occupied by the water molecule	The number of water molecules per 1 cm^2 of a monolayer	4×10^{14} cm^{-2}
ν	$(4-1.2)\times10^{19}$ cm^{-2} s^{-1}	Formulas (7), (11)	Initial concentrations of molecules in experiments, $(3-8)\times10^{15}$ cm^{-3}	Formula (11)
τ_{pa}	15–50 s	Formulas (12), (15), and (16). $\tau_{\mathrm{pa}}=N_{\mathrm{m}}/\alpha\nu$	Physical adsorption. A significant part of the centers is occupied by molecules captured via chemical adsorption. The fitting parameter is the probability of capture by vdW forces $\alpha=\alpha_0(1-\theta)=10^{-7}$	20–60 s depending on the concentration of water molecules in the tube. Formulas (12), (15), and (16)
τ_{pd}	$2\times(10^{-10}-10^{-11})$ s	[7], see also the text below formula (20)	$U_{\mathrm{d}}=0.14$ eV (depth of the vdW potential)	10^{-10} s
τ_{ca}	15–50 s	Similar to τ_{pa}	$\alpha_0^C=\alpha_0\exp(E_{\mathrm{a}}/kT)$, $E_{\mathrm{a}}=0.37$ eV [7]	Formulas (12), (15), and (16)
τ_{cd}	80–150 s	Calculation by formula (23)	$\tau_{\mathrm{cd}}\approx4\tau^{***}$	100±5 s
$g(T)$	$10^{-28}-10^{-27}$ cm^3	Formula (19)	$\alpha=10^{-7}$	$(4\pm0.3)\times10^{-28}$ cm^3
τ^{***}	20–35 s	Experimental data are processed by formulas (20), (22)	Values of dn/dt are obtained for $t=0-10$ s	25±3 s
	20–30 s	Experimental data are processed by formulas (21), (23)	$t=250-300$ s, $\tau_{\mathrm{cd}}=100$ s	
	20–30 s	Formulas (20), (22)	$\tau_{\mathrm{cd}}=100$ s	
τ^{*}		Formula (9)		$(1-2)\times10^{-10}$ s
τ^{**}		Formula (10)		$(1-2)\times10^{-10}$ s
τ'		Formula (30)		33±3 s
τ''		Formula (29)		208±10 s
τ'''		Formula (27)		28±2 s

7. BALANCE OF PARTICLES, GENERAL DISCUSSION

The proposed kinetic model and the obtained data on the rates of adsorption-desorption processes and the data on the fitting parameters make it possible to complement the experimental data on the particle concentrations in the gas phase with the data on the content of molecules in the near-wall layers formed by physical and chemical adsorption mechanisms. The results are illustrated by Figs. 4 and 5.

The measurement results and their processing reveal that, under the simultaneous action of physical and chemical adsorption mechanisms, the number of molecules held by the vdW forces is much smaller than the number of molecules bound to the surface by shared electrons. Chemical adsorption in the considered system, therefore, has priority over physical adsorption from the viewpoint of particle accumulation on the surface.

In the range of times close to the establishment time for a stationary gas composition, n_p is about $10^2-10^3\,\mathrm{cm}^{-2}$, while n_c is 11–12 orders of magnitude higher. Hence, physical adsorption centers are screened by chemically adsorbed molecules. This, in particular, can be seen in Figs. 4 and 5, when even at the very beginning of the adsorption process a sharp drop in the surface density occurs after the molecules are fed into an empty tube. In spite of the fact that the number of molecules adsorbed by the physical mechanism is small, these molecules cannot be disregarded. Although in the balance (4) $n_\mathrm{p} \ll n_\mathrm{c}$, characteristic times $\tau_\mathrm{pd} \ll \tau_\mathrm{cd}$ and $n_\mathrm{p}/\tau_\mathrm{pd}$, $n_\mathrm{c}/\tau_\mathrm{cd}$ in Eqs. (8) and (20) can be comparable since the concentration of particles in the gas phase is determined by the rates of tunneling of the molecules bound to the surface through the corresponding barriers. At the same time, all molecules in the gas, as well as in physical and chemical adsorption layers, participate in one closed cycle of particle circulation. Recall that, in accordance with Eqs. (6) and (24), to calculate the total number of particles in the volume of a tube, it is necessary to take into account the fact that the surface is not perfect and its area is γ times larger than the area of the ideal surface.

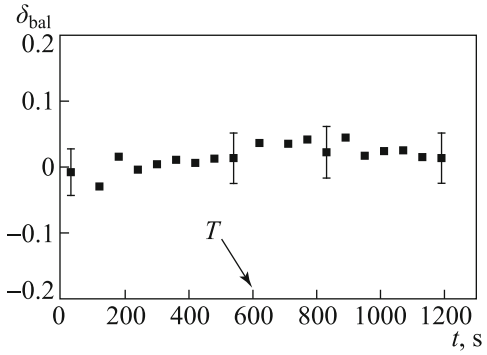

Fig. 6. Balance of the total number of water molecules in the gas, in the layers, and the molecules pumped out at time T. Results are averaged over $k = 15$ measurements.

Figure 6 shows the conservation of the total balance of particles, δ, normalized to the number of molecules introduced into an empty tube and averaged over all $k = 15$ measurement cycles. This balance also takes into account the exchange of particles in the layers, as well as in the gas, alongside with the particle removal from the tube (n_pump) resulting from intermediate pumping. The corresponding relation for the balance is

$$\delta_\mathrm{bal}(t) = \frac{1}{k}\sum_{i=1}^{k} \frac{n_0^i - n_\mathrm{exp}^i(t) - \gamma n_\mathrm{c}^i(t) - \gamma n_\mathrm{p}^i(t) - n_\mathrm{pump}^{T_i}}{n_0^i}. \tag{33}$$

It can be seen that the balance of the total number of particles (in the gas phase, in the layers, and the particles pumped out of the tube) is conserved with an accuracy of 4 to 5%. Note that in Figs. 4 and 5, the number of molecules in the layers is presented in units of surface density, while to compare the molecule concentrations n, one should consider γn_p and γn_c. The value $\gamma = 10$ not only corresponds to the balance condition (33) for the experiment but also agrees with the independently measured parameter τ^{***} (21). Here, under our experimental conditions, the concentration of chemically adsorbed particles γn_c turns out to be comparable or exceeds (at different stages of adsorption) the concentration of particles in the gas, n, and largely exceeds γn_p.

As mentioned above, expression (18), up to notations corresponds to the Langmuir isotherm (1). It is also a part of the kinetic equation (20). In our case, this situation is quite natural since the number of molecules bound by the vdW forces is small, and therefore, the complete monolayer N_m is not formed as the Langmuir theory suggests. The considered form of Eq. (20) arises since the size of the molecules of the chemical layer, n_c, is excluded from the kinetic equation (8) by substituting n_c from the balance condition (6) into (8). On the contrary, if we exclude n_p in the same way, then in the cases other than the considered one, instead of $N_\mathrm{m} g/(1+gn)$, isotherms (for example, (2), (3) with V replaced by n or other known isotherms) can be used in the equation of the type (16) to describe the dynamics of physical and chemical adsorption. At the same time, while maintaining the compatibility of the two mechanisms in the course of adsorption, the limits of applicability of the model can be extended since, for example, the BET isotherm, or the Freundlich isotherm, unlike the Langmuir isotherm, can be applied to multilayer physical and chemical adsorption as well. The validity

of these isotherms for stationary conditions was confirmed many times in numerous works. In this case, we assume that it is possible to use these isotherms to describe dynamic adsorption regimes. This assumption, however, requires additional research.

8. CONCLUSION

The dynamics of the concentrations of water molecules in a fused silica tube under reduced pressure 8×10^{15} to $10^{13}\,cm^{-3}$ was studied using diode laser spectroscopy. Two cases were considered: the case when water vapor fills the evacuated tube from the outside and the case of intermediate pumping when the molecules are released from the wall layers into the tube. In both cases, the observed dependences are non-exponential, and the indices of the corresponding power functions are determined by several processes with different characteristic times in a wide range 10^{-11} to 10^{2} s and also involving their combinations. A kinetic model of adsorption and desorption of particles held by van der Waals forces and chemical bonds was developed. The rate constants of reactions were matched so that the scheme well described the observed dynamics of molecules in the gas phase. Based on this model and the conditions of the particle balance, we established the changes in the surface densities of the adsorbates of both types over time. It was shown that under the considered conditions, the key role belongs to chemical adsorption. At the stage of dynamic equilibrium, the surface density of chemically adsorbed molecules is about $(2-4)\times10^{14}\,cm^{-2}$, which corresponds to approximately one monolayer per unit area of the geometric surface (without taking the roughness into account). For physically adsorbed particles, the surface density is 10^{2} to $10^{3}\,cm^{-2}$. Despite such a great difference, physically adsorbed molecules make a certain contribution to the formation of the gas phase in the volume. This contribution is comparable to that from desorption of chemically bound molecules since the molecules held by the van der Waals forces are characterized by small times of escape from the surface into the tube volume.

FUNDING

This work was supported by the Russian Scientific Foundation, Project 19-12-00310.

REFERENCES

1. J.W. McBain, "Der Mechanismus der Adsorption ("Sorption") von Wasserstoff durch Kohlenstoff," Z. Phys. Chem. **68U**(1), 471 (1909) [DOI: 10.1515/zpch-1909-6831].
2. J.H. de Boer, *The Dynamical Character of Adsorption* (Clarendon Press, Oxford, London, 1953).
3. S.J. Gregg and K.S.W. Sing, *Adsorption, Surface Area and Porosity* (Academic Press, London, N.Y., 1978).
4. S. Ross and J.P. Oliver, *On Physical Adsorption* (Wiley, N.Y., 1964).
5. L.N. Rozanov, *Vacuum Technique* (Taylor and Francis, London, N.Y., 2002).
6. L.N. Rozanov, "The Water Outgassing Rate of Internal Surfaces of Vacuum Systems," J. Phys.: Conf. Ser. **729**, 012001 (2016) [DOI: 10.1088/1742-6596/729/1/012001].
7. D.S. Sajko, V.V. Ganzha, S.A. Titov, A.V. Kostjuchenko, and S.A. Soldatenko, "Examination of Adsorption of Water on Crystal Vibrators. Experiment and a Physical Analog of Process," Cond. Matter Interphas. **10**(3), 249 (2008) [in Russian].
8. I. Sorokin, I. Vizgalov, K. Gutorov, and F. Podolyako, "Concerning Feasibility of Water Microleakage Diagnostics by Auto-oscillating Discharge," Phys. Proc. **71**, 116 (2015) [DOI: 10.1016/j.phpro.2015.08.324].
9. ITER Final Design Report No. G31 DDD 14 01_07-19 W0.1 (ITER Organization, St. Paul-lez-Durance, 2001). Sec. 3.1.
10. A.V. Bernatskiy, V.N. Ochkin, R.N. Bafoev, and A.B. Antipenkov, "Dynamics of the Water Molecule Density in a Discharge Chamber Filled with a Low-Pressure Humid Gas," Plasma Phys. Rep. **42**(10), 990 (2016) [DOI: 10.1134/S1063780X16100019].
11. A.V. Bernatskiy, V.N. Ochkin, O.N. Afonin, and A.B. Antipenkov, "Measurements of the Number Density of Water Molecules in Plasma by Using a Combined Spectral–Probe Method," Plasma Phys. Rep. **41**(9), 705 (2015) [DOI: 10.1134/S1063780X15090032].
12. A.V. Bernatskiy, V.N. Ochkin, I.V. Kochetov, "Multispectral Actinometry of Water and Water Derivative Molecules in Moist, Inert Gas Discharge Plasmas," J. Phys. D: Appl. Phys. **49**, 395204 (2016) [DOI: 10.1088/0022-3727/49/39/395204].
13. A.V. Bernatskiy and V.N. Ochkin, "Detection of Water Molecules in Inert Gas Based Plasma by the Ratios of Atomic Spectral Lines," Plasma Sources Sci. Technol. **26**, 015002 (2017) [DOI: 10.1088/0963-0252/26/1/015002].
14. S.N. Andreev, V.N. Ochkin, V.V. Zakharov, and S.Yu. Savinov, "Plasma-Chemical CO_2 Decomposition in a Non-Self-Sustained Discharge with a Controlled Electronic Component of Plasma," Spectrochim. Acta. Pt. A: Mol. Biomol. Spectrosc. **60**(14), 3361 (2004) [DOI: 10.1016/j.saa.2004.01.034].
15. I.V. Nikolaev, V.N. Ochkin, M.V. Spiridonov, and S.N. Tskhai, "Diode Ring-Down Spectroscopy without Intensity Modulation in an Off-Axis Multipass Cavity," Spectrochim. Acta. Pt. A: Mol. Biomol. Spectrosc. **66**(4–5), 832 (2007) [DOI: 10.1016/j.saa.2006.11.008].

16. V.N. Ochkin, S.Yu. Savinov, S.N. Tskhai, U. Czarnetzki, V.S. von der Gathen, and H.F. Dobele, "Nonlinear Optical Techniques for Plasma Diagnostics," IEEE Trans. Plasma Sc. **26**(5), 1502 (1998) [DOI: 10.1109/27.736047].
17. E.V. Parkevich, G.V. Ivanenkov, M.A. Medvedev, A.I. Khirianova, A.S. Selyukov, A.V. Agafonov, A.R. Mingaleev, T.A. Shelkovenko, and S.A. Pikuz, "Mechanisms Responsible for the Initiation of a Fast Breakdown in an Atmospheric Discharge," Plasma Sources Sci. Technol. **27**(11), 11LT01 (2018) [DOI: 10.1088/1361-6595/aaebdb].
18. E.V. Parkevich, M.A. Medvedev, A.S. Selyukov, A.I. Khirianova, A.R. Mingaleev, S.N. Mishin, S.A. Pikuz, and A.V. Oginov, "Setup Involving Multi-Frame Laser Probing for Studying Fast Plasma Formation with High Temporal and Spatial Resolutions," Opt. Lasers Eng. **116**, 82 (2019) [DOI: 10.1016/j.optlaseng.2018.12.014].
19. S. Brunauer, P.H. Emmett, and E. Teller, "Adsorption of Gases in Multimolecular Layers," J. Am. Chem. Soc. **60**(2), 309 (1937) [DOI: 10.1021/ja01269a023].
20. L.N. Rozanov, "Desorption Gas Discharge of Construction Vacuum Materials," Vakuumnaya Tekhnika i Tekhnologiya. **21**(3), 143 (2011) (www.vacuum.ru/cgi-bin/zurnal/go.cgi?rnd=9729308&file=2011-21-3-9729308.pdf) [in Russian].
21. L.N. Rozanov, "Degree of Coating Surface of Stainless Steel by Adsorbed Water Molecules at Low Pressure and Various Temperatures," Vakuumnaya Tekhnika i Tekhnologiya. **22**(4), 197 (2012) (www.vacuum.ru/cgi-bin/zurnal/go.cgi?rnd=1156616&file=2012-22-4-1156616.pdf) [in Russian].
22. A.V. Bernatskiy, V.V. Lagunov, and V.N. Ochkin, "Measurements of Water Molecule Isotopomer Concentrations in a Discharge of Inert Gas with Addition of H_2O and D_2 Vapours by the Method of External-Cavity Diode Laser Spectroscopy," Quantum Electronics **49**(2), 157 (2019) [DOI: 10.1070/QEL16819].
23. I.V. Nikolaev, V.N. Ochkin, G.S. Peters, M.V. Spiridonov, and S.N. Tskhai, "Recording Weak Absorption Spectra by the Phase-Shift Method with Deep Amplitude and Frequency Modulation Using a Diode Laser and a High Q Cavity," Laser Phys. **23**(3), 035701 (2013) [DOI: 10.1088/1054-660X/23/3/035701].
24. G. Gagliardi and H.P. Loock, *Cavity-Enhanced Spectroscopy and Sensing* (Springer, Berlin, 2014) [DOI: 10.1007/978-3-642-40003-2].
25. I.E. Gordon, L.S. Rothman, C. Hill, R.V. Kochanova, Y. Tan, P.F. Bernath, M. Birk, V. Boudon, A. Campargue, K.V. Chance, et al. "The HITRAN2016 Molecular Spectroscopic Database," J. Quant. Spectrosc. Rad. Transfer. **203**, 3 (2017) [DOI: 10.1016/j.jqsrt.2017.06.038].
26. N. Jacquinet-Husson, N.A. Scott, A. Chedin, L. Crepeau, R. Armante, V. Capelle, J. Orphal. A. Coustenis, C. Boonne, et al. "The GEISA Spectroscopic Database: Current and Future Archive for Earth and Planetary Atmosphere Studies," J. Quant. Spectrosc. Rad. Transfer. **109**(6), 1043 (2008) [DOI: 10.1016/j.jqsrt.2007.12.015].
27. http://spectra.iao.ru
28. V.N. Ochkin, *Spectroscopy of Low Temperature Plasma* (Wiley-VCH, N.Y., 2009).
29. V.N. Ochkin, "On the Errors in Measuring the Particle Density by the Light Absorption Method," Plasma Phys. Rep. **41**(4), 350 (2015) [DOI: 10.1134/S1063780X15040042].
30. Ya.B. Zel'dovich and A.D. Myshkis, *Elements of Applied Mathematics* (Mir, Moscow, 1976) [www.archive.org/details/ZeldovichMyskisElementsOfAppliedMathematics].
31. I.N. Bronshteyn and K.A. Semendyayev, *Handbook of Mathematics*, 4th ed. (Springer, Berlin, 2004).
32. S.R. Morrison, *The Chemical Physics of Surfaces* (Pienum Press, N.Y., London, 1977).
33. I. Ralph, *Chemistry of Silica—Solubility, Polymerization, Colloid and Surface Properties and Biochemistry* (Wiley-Interscience, N.Y., 1979)